ICASSP 2024 - 2024 IEEE International Conference on Acoustics, Speech and Signal Processing (ICASSP) | 979-8-3503-4485-1/24/$31.00 ©2024 IEEE | DOI: 10.1109/ICASSP48485.2024.10448252

PRACTICAL CHALLENGE AND SOLUTION FOR IRS-AIDED INDOOR LOCALIZATION SYSTEM

Ganlin Zhang[1], *Dongheng Zhang*[1*] , *Hongyu Deng*[2], *Yun Wu*[1], *Fengquan Zhan*[1], *and Yan Chen*[1]

[1]University of Science and Technology of China, Hefei, China
[2] Chinese University of Hong Kong, Hong Kong, China

ABSTRACT

Intelligent reflecting surfaces (IRS) is a novel integrated sensing and communication technology that can manipulate the propagation of wireless signals. However, existing IRS-based sensing systems require directional antennas for signal transmission, incompatible with commercial WiFi devices. This paper proposes an IRS-aided localization system using omnidirectional antennas and reveals two critical challenges in practical deployment. First, the accurate distance between the IRS and the transmitter is needed for IRS codebook design, but practice measurements invariably introduce centimeter-level bias, which seriously affects localization accuracy. We derive a linear relationship between measurement bias and localization error for calibration. Second, only relative IRS phase change under different bias voltages can be measurable, not the absolute phase offset, introducing an unknown fixed phase offset in reflections. We solve this challenge by eliminating the signals that are not related to the IRS. Experiments validate the proposed calibration techniques, proving that our system achieves high-precision passive localization.

Index Terms— Intelligent Reflecting Surface; Passive Indoor Localization; Omnidirectional Antennas; Calibration.

1. INTRODUCTION

Intelligent reflecting surface (IRS) [1–3] has been proposed as a potential method for supporting integrated sensing and communication, due to the ability to increase sensing capabilities [4,5] while improving wireless link quality [6,7]. It comprises a large number of inexpensive passive elements that can independently control incident signals. Several studies [8–11] developed IRS-aided localization and imaging systems, and use directional antennas for signal transmission and reception to ensure that most of the transmitted signals are reflected by the IRS. However, since commercial WiFi devices use omnidirectional antennas for full-house signal coverage, the reliance on directional antennas contradicts the philosophy of ISAC, limiting applicability. Thus, developing an IRS-aided sensing system with omnidirectional antennas is crucial but introduces challenges. With omnidirectional antennas, besides receiving the signal reflected by the IRS to the target, a stronger direct signal from the transmitter to the target is also received by the Rx, which needs to be considered in the IRS codebook design. Also, omnidirectional transmitter signals can directly reach other objects in the environment, increasing interference and complicating target sensing [12–14].

In this paper, we propose a prototype of an IRS-aided indoor localization system that utilizes omnidirectional antennas, as shown in Fig. 1. Furthermore, we reveal two practical challenges that emerge in practical deployment:

Accurate modeling of signal propagation. Existing work assumes known transceiver and IRS coordinates, essential for determining the IRS phase shift and achieving precise beam control. However, centimeter-level measurement bias between the transmitter and IRS is unavoidable in practice, which could cause localization errors of tens of centimeters or meters. We define this as *inaccurate Tx position*. Analysis reveals a linear relationship between measurement biases and localization errors, which can be utilized to calibrate the Tx position based on the target's localization error.

Mitigating the IRS unknown phase offset. Second, measuring the relationship between reflection coefficients and bias voltages of the IRS is crucial for precise control. However, the true phase shift (ϕ_{xV}) at each voltage cannot be directly measured. Instead, only the relative phase change ($\phi_{xV} - \phi_{0V}$) with respect to a 0V reference is measurable, while the absolute offset (ϕ_{0V}) at 0V remains unknown [15, 16]. We define this as *unknown phase offset problem*, which introduces a fixed unknown offset in the channel response of IRS-aided signals. This prevents obtaining the accurate phase difference between the IRS-aided path and the Tx-Target-Rx path, impacting IRS codebook design. To solve this problem, we divide the received signal into two parts according to whether it is reflected by the IRS, then remove the received signal that is irrelevant to the IRS and only keep the IRS reflected signal.

Real-world experiments validate the accuracy of our theoretical analysis, and demonstrate the effectiveness of our calibration techniques, proving that our system can achieve accurate passive localization.

Corresponding author: Dongheng Zhang. This work was supported by Anhui Key R&D Programmes under Grant 2022h11020026, National Key R&D Programmes under Grant 2022YFC2503405 and 2022YFC0869800.

2. LOCALIZATION MODEL

As illustrated in Fig. 1, the proposed IRS-aided localization system comprises a single-antenna transmitter (Tx), an IRS with I reflecting elements, and a four-antenna receiver (Rx). With an omnidirectional transmit antenna, the signal reflected by the target can be categorized into Tx-Target-Rx and IRS-aided paths. The Tx-Target-Rx path propagates from Tx to target to Rx. The IRS-aided path reaches the IRS first before reflecting to the target and Rx. The signal reflected by the target can be expressed as $y^n_{target} = y^n_{Tx-Target-Rx} + y^n_{IRS-aided} = \alpha \cdot e^{-j2\pi(d_{TO}+d^n_{OR})/\lambda} + \sum_{i=1}^{I} \alpha_i \cdot e^{-j2\pi(d_{TI_i}+d_{I_iO}+d^n_{OR})/\lambda e^{j\phi^i}}$, where d_{TO} is the distance between the Tx and the target, d^n_{OR} is the distance between the target and the n-th Rx, d_{TI_i} is the distance from the Tx to the i-th IRS element, d_{I_iO} is the distance from the i-th IRS element to the target, α and α_i are the attenuation factor for the Tx-Target-Rx path and i-th IRS-aided path, respectively.

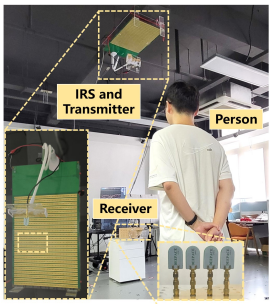

Fig. 1: The IRS-aided indoor localization system. Both the Tx and Rx are omnidirectional.

In practical indoor environments, besides the signal reflected by the target, the received signal also contains multipath reflections from walls and furniture. To remove static multipath components, the localization model [17] first gathers the reference signal y_0 from the empty environment. Since static multipaths are time-invariant, it is removed by subtracting the received signal during localization from y_0. Then, the localization model [17,18] uses the maximum received signal power to detect the target location. Specifically, the indoor space is discretized into A blocks. For each block O_a, the optimal phase shift of IRS is

$$\phi^{*,i}_{o_a} = \frac{2\pi(d_{TI_i} + d_{I_iO_a} - d_{TO_a})}{\lambda_k}, \quad i = 1, \ldots, I. \qquad (1)$$

The block with the highest energy is the target location. For more details on the localization model, please refer to [17,18].

3. PRACTICAL CHALLENGES

3.1. Problem 1: Inaccurate Tx Position

In the localization model, a precise distance between the Tx and IRS is necessary for calculating the optimal phase shift.

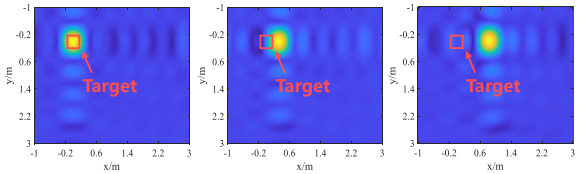

(a) (b) (c)

Fig. 2: Simulated results of the localization model under different Tx measurement biases. (a) zero bias causes zero localization error; (b) 0.05 m bias causes 0.32 m error; (c) 0.13 m bias causes 0.84 m error.

However, centimeter-level measurement biases often occur in practice. For a typical configuration with a large IRS near the Tx, the measurement bias in the Tx-IRS distance has a non-negligible impact on the localization results. We conduct simulations for a better demonstration of this challenge. Fig. 2 shows the localization results under different measurement biases Δx. With $\Delta x = 0$ m, the block with the strongest signal coincides with the actual position of the target. However, 0.05 m and 0.13 m biases cause 0.32 m and 0.84 m localization errors. Even minor measurement biases can thus cause substantial decimeter-to-meter errors. We undertake an analysis to further examine this issue.

First, we analyze the 2D scenario, as shown in Fig. 3. The vertical distance between the Tx to the IRS is z_0, while the distance from the target to the Tx is z_1. The true location of the Tx is at $(0, 0)$. Due to a measurement bias Δx along the X-axis, the obtained erroneous Tx position is $(\Delta x, 0)$. The i-th IRS element I_i is positioned at $(x_i, -z_0)$, with the target at $(0, z_1)$.

Since the signal propagation distances between the Tx-Target-Rx path and the IRS-aided path differ, according to (1), the ideal distance to be compensated is $d_i = d_{TI_i} + d_{I_iO} - d_{TO} = \sqrt{{x_i}^2 + {z_0}^2} + \sqrt{{x_i}^2 + (z_0 + z_1)^2} - z_1$. Due to the Tx position measurement bias, the distance calculated based on the erroneous Tx' is $d'_i = d_{T'I_i} + d_{I_iO} - d_{T'O} = \sqrt{(x_i - \Delta x)^2 + {z_0}^2} + \sqrt{{x_i}^2 + (z_0 + z_1)^2} - \sqrt{\Delta x^2 + {z_1}^2}$. The result of subtracting d_i from d'_i is $\Delta d_i = (d_{TI_i} - d_{T'I_i}) - (d_{TO} - d_{T'O}) = (\sqrt{{x_i}^2 + {z_0}^2} - \sqrt{(x_i - \Delta x)^2 + {z_0}^2}) - (z_1 - \sqrt{\Delta x^2 + {z_1}^2})$. The phase shift calculated based on the erroneous Tx does not match the ideal value. Moreover, the discrepancy differs across IRS elements, with some under-compensated and others over-compensated. Therefore, the reflected energy at the target position is not maximized, and a bright spot does not appear at the target position.

However, Fig. 2 shows a bright spot appearing at a different location O' where no target exists. This indicates that the calculated distance $d'_{O',i}$ at location O' equals the ideal value $d_{O,i}$, causing coherent superposition of signals. The coordinates of O', represented as (x_e, z_1), must fulfill the following requirement: $\sqrt{{x_i}^2 + {z_0}^2} + \sqrt{{x_i}^2 + (z_0 + z_1)^2} - z_1 = \sqrt{(x_i - \Delta x)^2 + {z_0}^2} + \sqrt{(x_i - x_e)^2 + (z_0 + z_1)^2} -$

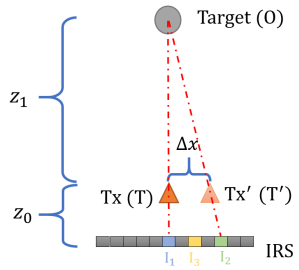

Fig. 3: In the 2D model, a centimeter-scale measurement bias Δx arises when measuring the Tx coordinates. The calculated phase shift for the IRS codebook deviates from the ideal value, causing significant localization errors.

$\sqrt{(\Delta x - x_e)^2 + {z_1}^2}$, $i = 1, \ldots, M$. Since z_1 is significantly larger than z_0 and x_i, we simplify the expression and obtain the approximate position of O' as

$$x_e \approx -\frac{z_1}{z_0}\Delta x \tag{2}$$

As a result, the calculated IRS phase shift at $(-\frac{z_1}{z_0}\Delta x, z_1)$, where no target exists, equals the ideal value, resulting in a bright spot appearing at this position. Importantly, the localization error is proportional to the measurement bias, with proportionality factor $-\frac{z_1}{z_0}$. Given the substantial disparity between z_1 and z_0, even a small measurement bias of a few centimeters can cause a significant localization error.

In the 3D scenario with 2D IRS, we can get a similar result, with the false target location being $x_e \approx -\frac{z_1}{z_0}\Delta x, y_e \approx -\frac{z_1}{z_0}\Delta y$, and the impact of Δz on the localization result can be neglected. It can be seen that the measurement bias along the X-axis only causes localization errors in the X direction, while Y-axis measurement bias only causes Y-direction localization errors. Moreover, even if the target is not at the coordinate origin but at (x_1, y_1, z_1), the previous results are valid as long as $z_1 \gg x_1, y_1$, and the result is $(x_1 - \frac{z_1}{z_0}\Delta x, y_1 - \frac{z_1}{z_0}\Delta y, z_1)$.

Calibration of Tx position is imperative before employing the IRS-aided system. The analysis reveals a linear relationship between the localization error and measurement bias in each dimension (X-axis, Y-axis), with proportionality coefficient $-z_1/z_0$. Thus, given the known localization error x_e, y_e and the parameter $-z_1/z_0$, the measurement bias can be deduced. Specifically, the calibration procedure is: **1)** Position the target at $(0, 0, z_1)$, initialize the Tx position to $(0, 0, 0)$, and set the vertical distance between the IRS and the Tx as $-z_0$; **2)** Localize the target, and obtain the result (x_e, y_e, z_1); **3)** Calculate the measurement biases $\Delta x = -x_e \times \frac{z_0}{z_1}$ and $\Delta y = -y_e \times \frac{z_0}{z_1}$; **4)** Update the Tx position to $(-\Delta x, -\Delta y, 0)$. Besides, new noises may occur when measuring z_0, z_1, and target location $(0, 0, z_1)$ during calibration. However, we find both theoretically and experimentally that the effect of these noises on the calibration accuracy is negligible by placing the target sufficiently far from the Tx.

3.2. Problem 2: Unknown Phase Offset

Controlling the IRS requires knowing the relationship between the bias voltage and phase shift of the IRS, often obtained via simulation with software such as the CST Microwave Studio software or the Ansys HFSS. However, unavoidable discrepancies often exist between the simulated and actual IRS elements due to non-ideal characteristics [15,16,19]. To enable precise control, prior works [15,16] measure this relationship in the microwave anechoic chamber. In fact, the IRS phase information contains two parts: one is the phase offset by the IRS itself, which is the phase shift at zero voltage, and the other is the relative phase change under different voltages. Unfortunately, the measurement results [15, 16] only provide the relative phase shift between different voltages, while accurately measuring the ϕ_{0V} is challenging. The phase of the received signal depends on both the propagation path and IRS phase shift. Small errors in measuring the Tx-IRS and IRS-Rx distances cause substantial deviation in ϕ_{0V}, termed *the unknown phase offset*.

In practice, since the absolute phase shift at each voltage is needed to apply appropriate control, the phase offset at 0V must be assumed in advance, e.g. 0°. However, this assumption often deviates from the real offset, which we define the difference as $\Delta\phi_{0V}$. Thus, each IRS element will overcompensate the phase shift by $\Delta\phi_{0V}$ compared to the theoretically optimal value calculated from (1). With directional antennas, the offset is identical across elements so the IRS-aided signals still combine coherently, maintaining model validity despite the problem. However, with omnidirectional antennas, not all signals are reflected by the IRS before reaching the target. Thus, a phase difference $\Delta\phi_{0V}$ exists between the Tx-Target-Rx path and the IRS-aided path, impeding coherent combining. Especially if $\Delta\phi_{0V}$ is 180°, the IRS-aided signal destructively interferes with the Tx-Target-Rx signal at the target location, causing low received signal power and maximum localization error.

Thus, the unknown phase offset problem must be addressed before system deployment. The analysis reveals that this problem only prevents phase alignment between the Tx-target-Rx path and IRS-aided path, while the reflected signals between IRS elements remain phase-coherent. Therefore, we only need to eliminate the Tx-target-Rx path from the received signals, retaining only the IRS-aided component. We utilize the characteristic that the signal of the Tx-Target-Rx path does not change with different IRS codebooks, to collect two groups of signals with opposite IRS phase shifts (Codebook $\mathbb{A}$ and Codebook $\mathbb{B}$) in advance, and then separate the Tx-Target-Rx path signal from them. In Codebook $\mathbb{A}$, the phase shifts of each IRS element are randomly generated. In Codebook $\mathbb{B}$, the phase of each element is obtained by adding 180° to the corresponding phase in Codebook $\mathbb{A}$. The signal reflected by the target with Codebook $\mathbb{A}$ can be expressed as $y_a =$

$y_{Tx-Target-Rx} + \sum_{i=1}^{I} \alpha_i \cdot e^{-j(\phi^i_{distance}+\phi_{0V}+\Delta\phi^i)}$ where $\phi^i_{distance} = 2\pi(d_{TI_i} + d_{I_iO} + d^n_{OR})/\lambda$. The signal reflected by the target with Codebook $\mathbb{B}$ can be expressed as $y_b = y_{Tx-Target-Rx} + \sum_{i=1}^{I} \alpha_i \cdot e^{-j(\phi^i_{distance}+\phi_{0V}+\Delta\phi^i+\pi)} = y_{Tx-Target-Rx} - \sum_{i=1}^{I} \alpha_m \cdot e^{-j(\phi^i_{distance}+\phi_{0V}+\Delta\phi^i)}$. Thus, the signal of the Tx-Target-Rx path can be calculated by $y_{Tx-Target-Rx} = (y_a + y_b)/2$. In the subsequent localization process, we subtract the calculated Tx-Target-Rx path signal from the received signal of each block to extract the IRS-aided signal. This method avoids the difficulty of directly measuring the IRS phase offset and provides a feasible solution to the unknown phase offset problem.

4. EXPERIMENTAL VERIFICATION

Localizing Corner Reflector. We first present the localization results in an indoor environment with a corner reflector. The Tx is placed 0.3 m from the IRS. The designed IRS consists of 8×8 super unit cells, each with 9 concurrently stimulated elements. By adjusting the bias voltage applied to the varactor diode, each cell generates different reflection phase shifts. The target is on the X-Y plane, 2 meters from the Tx.

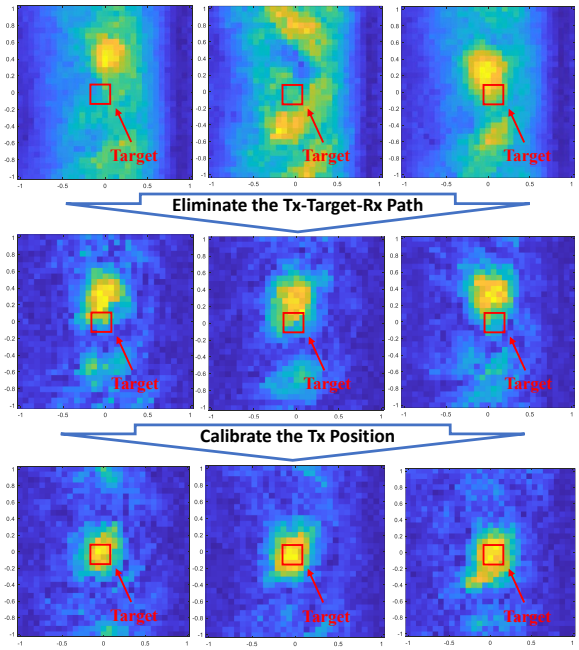

Fig. 4: Localization results for the same target position before and after solving the unknown phase offset and calibrating Tx position under three different assumed ϕ_{0V} (0°, 120°, 240°).

First, we verify the impact of the unknown phase offset problem using three experiments with different assumed phase offsets on the same target. As shown in the first row of results of Fig. 4, localization result varies for the assumed phase offsets. We then apply our proposed solution in Section 3.2 to eliminate the unknown phase offset. As shown in the second row of Fig. 4, subtracting the $y_{Tx-Target-Rx}$ from the received signal provides consistent localization for the three assumed ϕ_{0V}. This demonstrates our solution effectively resolves the unknown phase offset problem.

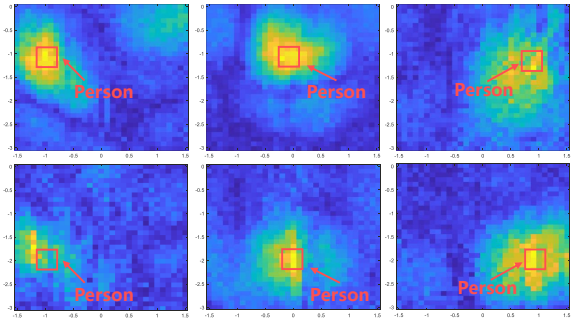

Fig. 5: Localization results of our proposed IRS-aided system when the person is in six different locations.

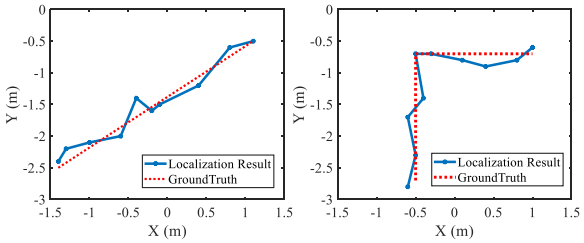

Fig. 6: The comparison between the extracted human trajectories and the ground truth in two scenarios.

However, the localization results of the three assumed phase offsets do not match the actual target position $(0, 0)$. This is due to inaccurate Tx-IRS distance measurement. The localization error of 0.3 m on the Y-axis indicates a 0.045 m ($0.3 \times 0.3/2$) measurement bias. Using the updated Tx position $(0, 0.045, 0)$, the recalculated localization results in the third row of Fig. 4 accurately match the target position, validating the effectiveness of our calibration method.

Localizing Human Target. Next, we evaluate the performance of human localization. Fig. 5 and Fig. 6 show the localization results for the person after addressing the unknown phase offset and the inaccurate Tx position. Our IRS-aided system achieves accurate human localization with an average error of 0.11 meters.

5. CONCLUSION

In this paper, we designed a novel IRS-aided localization system with omnidirectional transmit/receive antennas and tackled two major practical challenges. First, the inaccurate Tx position problem is calibrated based on the linear relationship between measurement bias and localization error. Second, the unknown phase offset problem is mitigated by extracting and eliminating the signal irrelevant to the IRS. Experiments demonstrated our proposed solutions overcame these challenges and enabled accurate indoor localization.

6. REFERENCES

[1] Samith Abeywickrama, Rui Zhang, Qingqing Wu, and Chau Yuen, "Intelligent reflecting surface: Practical phase shift model and beamforming optimization," *IEEE Transactions on Communications*, vol. 68, no. 9, pp. 5849–5863, 2020.

[2] Ying He, Dongheng Zhang, and Yan Chen, "High-resolution wifi imaging with reconfigurable intelligent surfaces," *IEEE Internet of Things Journal*, vol. 10, no. 2, pp. 1775–1786, 2022.

[3] Ziyi Wang, Zhenyu Liu, Yuan Shen, Andrea Conti, and Moe Z Win, "Location awareness in beyond 5G networks via reconfigurable intelligent surfaces," *IEEE Journal on Selected Areas in Communications*, vol. 40, no. 7, pp. 2011–2025, 2022.

[4] Ganlin Zhang, Dongheng Zhang, Ying He, Jinbo Chen, Fang Zhou, and Yan Chen, "Passive human localization with the aid of reconfigurable intelligent surface," in *2023 IEEE Wireless Communications and Networking Conference (WCNC)*. IEEE, 2023, pp. 1–6.

[5] Moritz Garkisch, Vahid Jamali, and Robert Schober, "Codebook-based user tracking in irs-assisted mmwave communication networks," in *ICASSP 2023-2023 IEEE International Conference on Acoustics, Speech and Signal Processing (ICASSP)*. IEEE, 2023, pp. 1–5.

[6] Boya Di, Hongliang Zhang, Lingyang Song, Yonghui Li, Zhu Han, and H. Vincent Poor, "Hybrid beamforming for reconfigurable intelligent surface based multi-user communications: Achievable rates with limited discrete phase shifts," *IEEE Journal on Selected Areas in Communications*, vol. 38, no. 8, pp. 1809–1822, 2020.

[7] Farjam Karim, Bishmita Hazarika, Sandeep Kumar Singh, and Keshav Singh, "A performance analysis for multi-ris-assisted full duplex wireless communication system," in *ICASSP 2022-2022 IEEE International Conference on Acoustics, Speech and Signal Processing (ICASSP)*. IEEE, 2022, pp. 5313–5317.

[8] Tao Shan, Xiaotian Pan, Maokun Li, Shenheng Xu, and Fan Yang, "Coding programmable metasurfaces based on deep learning techniques," *IEEE journal on emerging and selected topics in circuits and systems*, vol. 10, no. 1, pp. 114–125, 2020.

[9] Henk Wymeersch, Jiguang He, Benoit Denis, Antonio Clemente, and Markku Juntti, "Radio localization and mapping with reconfigurable intelligent surfaces: Challenges, opportunities, and research directions," *IEEE Vehicular Technology Magazine*, vol. 15, no. 4, pp. 52–61, 2020.

[10] Lianlin Li, Hengxin Ruan, Che Liu, Ying Li, Ya Shuang, Andrea Alù, Cheng-Wei Qiu, and Tie Jun Cui, "Machine-learning reprogrammable metasurface imager," *Nature communications*, vol. 10, no. 1, pp. 1–8, 2019.

[11] Mingtuan Lin, Ming Xu, Xiang Wan, Hanbing Liu, Zhaofeng Wu, Jibin Liu, Bowen Deng, Dongfang Guan, and Song Zha, "Single sensor to estimate DOA with programmable metasurface," *IEEE Internet of Things Journal*, vol. 8, no. 12, pp. 10187–10197, 2021.

[12] Dongheng Zhang, Yang Hu, and Yan Chen, "Mtrack: Tracking multiperson moving trajectories and vital signs with radio signals," *IEEE Internet of Things Journal*, vol. 8, no. 5, pp. 3904–3914, 2020.

[13] Dongheng Zhang, Yang Hu, Yan Chen, and Bing Zeng, "BreathTrack: Tracking indoor human breath status via commodity WiFi," *IEEE Internet of Things Journal*, vol. 6, no. 2, pp. 3899–3911, 2019.

[14] Zhi Wu, Dongheng Zhang, Chunyang Xie, Cong Yu, Jinbo Chen, Yang Hu, and Yan Chen, "Rfmask: A simple baseline for human silhouette segmentation with radio signals," *IEEE Transactions on Multimedia*, 2022.

[15] Jun Yan Dai, Wan Kai Tang, Jie Zhao, Xiang Li, Qiang Cheng, Jun Chen Ke, Ming Zheng Chen, Shi Jin, and Tie Jun Cui, "Wireless communications through a simplified architecture based on time-domain digital coding metasurface," *Advanced materials technologies*, vol. 4, no. 7, pp. 1900044, 2019.

[16] Xilong Pei, Haifan Yin, Li Tan, Lin Cao, Zhanpeng Li, Kai Wang, Kun Zhang, and Emil Björnson, "RIS-aided wireless communications: Prototyping, adaptive beamforming, and indoor/outdoor field trials," *IEEE Transactions on Communications*, vol. 69, no. 12, pp. 8627–8640, 2021.

[17] Ganlin Zhang, Dongheng Zhang, Ying He, Jinbo Chen, Fang Zhou, and Yan Chen, "Multi-person passive WiFi indoor localization with intelligent reflecting surface," *IEEE Transactions on Wireless Communications*, pp. 1–1, 2023.

[18] Chao Feng, Xinyi Li, Yangfan Zhang, Xiaojing Wang, Liqiong Chang, Fuwei Wang, Xinyu Zhang, and Xiaojiang Chen, "Rflens: metasurface-enabled beamforming for iot communication and sensing," in *Proceedings of the 27th Annual International Conference on Mobile Computing and Networking*, 2021, pp. 587–600.

[19] Jun Yang, Yijian Chen, Yijun Cui, Qingqing Wu, Jianwu Dou, and Yuxin Wang, "How practical phase-shift errors affect beamforming of reconfigurable intelligent surface?," *arXiv preprint arXiv:2304.06388*, 2023.